JOURNAL OF MATERIALS SCIENCE 26 (1991) 3244–3248

A precipitate phase in AA2124

YAN JIN, CHUNZHI LI, MINGGAO YAN
Institute of Aeronautical Materials, Beijing, 100095, and Laboratory of Solid Atomic Images, Institute of Metals, Academic Sinica, Shenyang, People's Republic of China

A new precipitate phase (designated X phase) other than the S(Al_2CuMg) precipitate phase has been discovered in the 2124 aluminium alloy. Using selected-area electron diffraction analysis, dynamical diffraction simulation, energy dispersion analysis of X-rays and high-resolution electron microscopy, it is suggested that the X phase has an orthorhombic crystal structure with $a = 0.492$ nm, $b = 0.852$ nm and $c = 0.701$ nm. The space group of the phase is Cmmm. There are 10 atoms in a cell with Al : Cu : Mg = 2 : 4 : 4. The orientation relationship between the X phase and the matrix is determined as $(1\ -1\ 0)_m \| (0\ 1\ 0)_x$, $[-1\ -1\ -1]_m \| [0\ 0\ 1]_x$.

1. Introduction

The 2124 aluminium alloy is one of the most commonly used age-hardening Al–Cu–Mg alloys. Therefore, research on the precipitate phases in the alloy is quite important. Until now, most researchers [1–5] believed that only S(Al_2CuMg) precipitate existed in AA2124. The S phase has an orthorhombic crystal structure with $a = 0.400$ nm, $b = 0.923$ nm and $c = 0.714$ nm [4, 5]. The orientation relationship between the matrix and S phase is $(1\ 0\ 0)_m \| (1\ 0\ 0)_s$, $[0\ 1\ 2]_m \| [0\ 0\ 1]_s$, where m and s indicate matrix and S phase, respectively. The S′ phase is the metastable phase of S phase. The orientation relationship between the matrix and S′ phase is similar to that of S phase. The ageing sequence of S phase can be written as GP zone → S′ phase → S phase.

In the present work, we observed another kind of orthorhombic precipitate phase with lattice parameters and atomic composition which are different from those of S precipitate phase. The ageing process of the phase has also been studied.

2. Experimental procedure

The alloys studied were laboratory melt-made to the specification of AA2124. The chemical composition of the experimental 2124 aluminium alloy was 4.9 wt % Cu, 1.8 wt % Mg, 0.9 wt % Mn, 0.3 wt % Fe and 0.2 wt % Si. The size of heat-treated specimens was 20 mm × 20 mm × 40 mm. The specimens were solution-treated at 495 °C for 90 min, water-quenched, then aged at different ageing temperatures shown in Table I.

The samples for observation were prepared with a conventional jet-polishing technique. The electrolyte contained one part of HNO_3 and three parts of CH_3OH (by volume). Observations by conventional transmission electron microscopy (TEM) was performed using an H-800 transmission electron microscope, and high-resolution electron microscopy (HREM) was performed using a JEM-200CX transmission electron microscope. The accelerating voltage was 200 kV in all cases. The orientation relationship between the matrix and precipitate phase was calculated using the method suggested by Li *et al.* [6]. The software for simulation of lattice images and dynamical diffraction patterns was provided by the Beijing Laboratory of Electron Microscopy.

3. Results and discussion

For convenience, we have called the new precipitate phase, X phase.

3.1. Lattice structure of X phase

Fig. 1 is the bright-field image of X phase in specimen A along the $[0\ 0\ 1]_m$ direction. The X phase appears as a bulk-like precipitate with different sizes. The selected-area electron diffraction (SAD) patterns of X phase along $[0\ 0\ 1]_m$, $[0\ 1\ 1]_m$ and $[1\ 1\ 2]_m$ directions are shown in Fig. 2. The corresponding parameters of the two-dimensional unit cell were measured and are listed in Table II, where R_1 and R_2 represent the lengths of the shortest and second-shortest reciprocal lattice vectors respectively, θ is the angle between them, and D_1 is the measured plane-spacing corresponding to R_1.

Through computer calculation, it was found that there were three possible lattice structures: (a) orthorhombic lattice, C-centred cell, $a = 0.492$ nm, $b = 0.852$ nm and $c = 0.701$ nm, (b) monoclinic lattice, primitive cell, $a = b = 0.492$ nm, $c = 0.701$ nm, $\gamma = 120°$. (c) Hexagonal lattice, primitive cell, $a = 0.492$ nm, $c = 0.701$ nm. The corresponding calculated parameters are listed in Table III.

TABLE I Heat treatment of the specimens

No.	Ageing-treatment
A	420 °C/2 h
B	190 °C/12 h
C	220 °C/12 h

0022–2461/91 $03.00 + .12

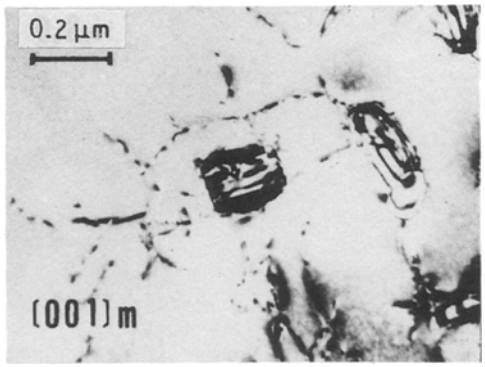

Figure 1 Bright-field image of X phase in specimen A along the $[0\,0\,1]_m$ direction.

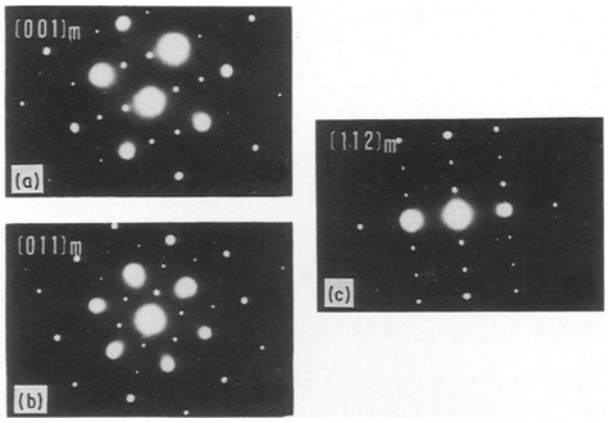

Figure 2 SAD patterns of X phase along (a) $[0\,0\,1]_m$, (b) $[0\,1\,1]_m$ and (c) $[1\,1\,2]_m$ directions.

TABLE II The reciprocal lattice parameters of two-dimensional unit cell corresponding to Fig. 2

No.	$[U\,V\,W]_m$	X phase		
		θ(deg)	R_2/R_1	D_1(nm)
(a)	$[0\,0\,1]_m$	72(108)	1.56	0.426
(b)	$[0\,1\,1]_m$	67(113)	1.18	0.426
(c)	$[1\,1\,2]_m$	90	1.83	0.426

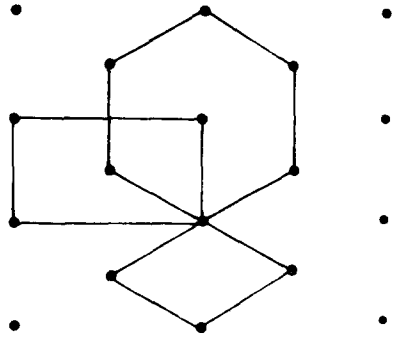

Figure 3 Schematic illustration of the three possible lattice cells mentioned in Table III.

The relationship between the three possible lattice cells is schematically illustrated in Fig. 3. Obviously, these three lattices have quite similar lattice structures and could hardly be distinguished using SAD analysis. Therefore, a further study using high-resolution electron microscopy (HREM) is necessary.

3.2. Crystal structure of X phase

Fig. 4 shows the EDAX analysis of the atomic composition of X phase in specimen A. The corresponding data are shown in Table IV. It was found that the X phase contains mainly Al, Cu and Mg. A small amount of Mn and Fe may also be present. From the experimental results, the ratio between Cu and Mg atoms in the X phase was calculated as 1:0.891. Owing to the influence of the Al matrix, the atomic composition of Al in the phase could not be determined. Because the average ratio between Cu and Mg atoms in the studied alloy is 1:0.978, the most probable atomic composition of X phase would be Al_xCuMg. Fig. 5 shows the lattice image of X phase in specimen A along the $[1\,1\,2]_m$ direction. If the X phase has the orthorhombic crystal structure, the corresponding direction of X phase would be $[1\,0\,2]_X$.

Considering the possibility of the orthorhombic crystal structure, observed along the $[0\,0\,1]_m$ matrix

TABLE III The reciprocal lattice parameters of two-dimensional unit cell calculated according to different lattice structures

No.	Lattice	R_2/R_1	θ(deg)	D_1(nm)	$H_1\,K_1\,L_1$	$H_2\,K_2\,L_2$	$U\,V\,W$
(a)	Orthorhombic	1.17	115.3	0.4260	0 2 0	−1 −1 1	1 0 1
	C-centred unit cell	1.17	115.3	0.4261	1 1 0	−1 1 1	1 −1 2
		1.57	108.3	0.4260	1 1 0	0 −2 −2	1 −1 1
		1.57	71.47	0.4260	0 −2 0	1 −1 −2	2 0 1
		1.84	90.00	0.4260	0 −2 0	2 0 −1	1 0 2
(b)	Monoclinic	1.17	64.71	0.4261	−1 −1 0	−1 0 1	1 1 1
	Primitive	1.17	64.71	0.4261	0 1 0	−1 1 1	1 0 1
	unit cell	1.57	71.48	0.4261	−1 1 0	−1 0 2	2 2 1
		1.57	108.5	0.4261	0 1 0	−1 0 2	2 0 1
		1.57	108.5	0.4261	0 1 0	−1 0 −2	−2 0 1
		1.84	90.00	0.4261	−1 1 0	−1 −1 1	1 1 2
		1.84	90.00	0.4261	0 1 0	−2 1 1	1 0 2
(c)	Hexagonal	1.17	115.3	0.4261	1 0 0	−1 1 1	0 1 −1
	Primitive	1.57	71.48	0.4261	1 0 0	0 1 2	0 −2 1
	unit cell	1.84	90.00	0.4261	1 0 0	−1 2 1	0 −1 2

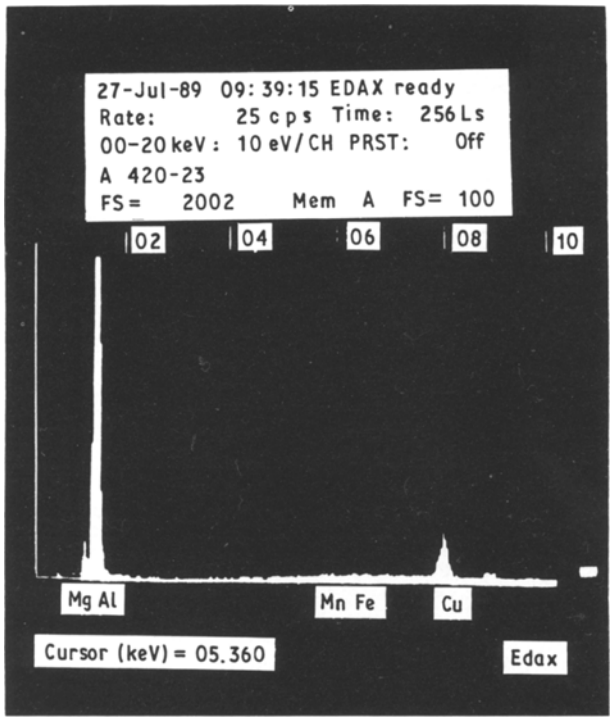

Figure 4 EDAX analysis of X phase in specimen A.

TABLE IV EDAX data of the atomic composition of the X phase

Element	CPS	Element (at %)
Mg	0.872	3.847
Al	161.729	90.921
Mn	1.327	0.449
Fe	1.463	0.421
Cu	17.384	4.361

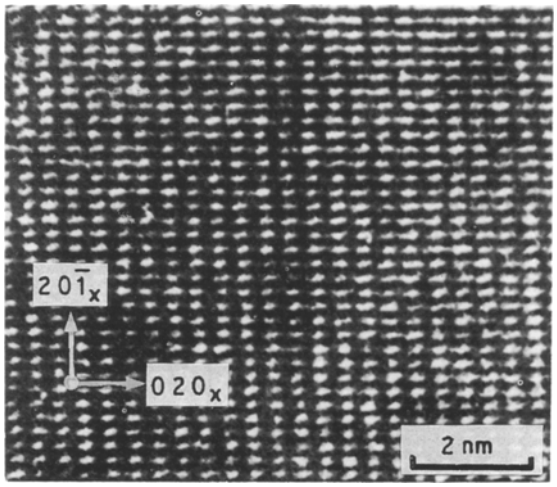

Figure 5 Lattice image of X phase in specimen A along the $[1\,1\,2]_m$ direction.

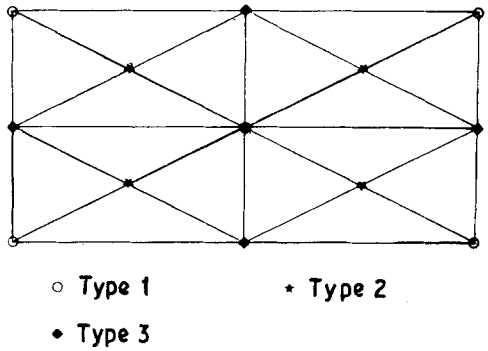

Figure 6 Equivalent atomic positions in a unit cell of X phase.

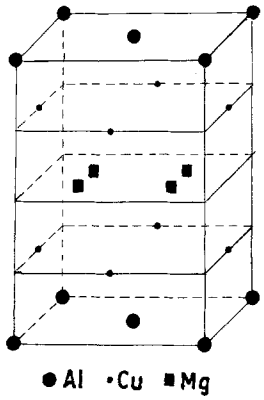

Figure 7 Crystal structure of X phase proposed by the authors.

direction, there would be three types of equivalent atomic positions in a unit cell as illustrated in Fig. 6. Because the most probable atomic composition of X phase is Al_xCuMg, the accurate atomic structure of X phase could be determined by assuming a series of crystal structures with different Al composition, and comparing the simulated lattice images with the observed lattice images, and the simulated dynamical diffraction pattern with the observed diffraction pattern. Therefore, we have proposed a crystal structure as schematically illustrated in Fig. 7. There are 10 atoms in total in a cell, with Al : Cu : Mg = 2 : 4 : 4. The atomic positions of each atom are listed in Table V, where the XA, YB and ZC represent the coordinates of each atom along the ***a***, ***b*** and ***c*** directions, respectively. The space group is Cmmm.

Using the software mentioned in the previous section, we have simulated the atomic images and the dynamical diffraction pattern of X phase, according to the proposed model. Fig. 8 shows the simulated images of X phase along the $[1\,0\,2]_X$ direction. In the thickness range 4.5–6.0 nm and the defocus range 10–30 nm, the simulated images changed little and are

TABLE V The atomic position of each atom in the proposed model of X phase

	1	2	3	4	5	6	7	8	9	10
Atom type	Al	Al	Cu	Cu	Cu	Cu	Mg	Mg	Mg	Mg
XA	0	0.5	0	0.5	0	0.5	0.25	0.25	0.75	0.75
YB	0	0.5	0.5	0	0.5	0	0.25	0.75	0.25	0.75
ZC	0	0	0.25	0.25	0.75	0.75	0.5	0.5	0.5	0.5

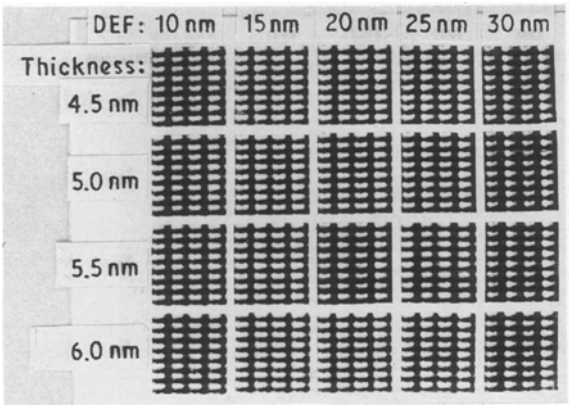

Figure 8 Simulated lattice images of X-phase according to the crystal model proposed in Fig. 7.

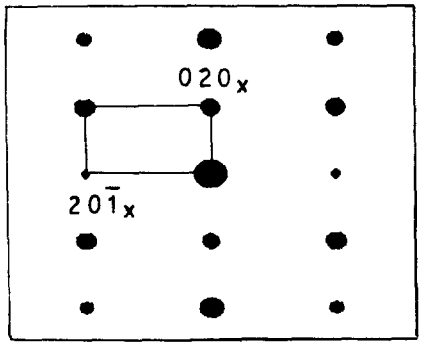

Figure 9 Simulated dynamical diffraction pattern of X phase according to the model proposed in Fig. 7.

all very similar to the experimental results. However, the image with defocus 20 nm and thickness $t = 5.5$ nm seems nearest to the observed image. Fig. 9 is the simulated dynamical diffraction pattern of X phase along $[1\,0\,2]_X$ direction. The assumed sample thickness is 5.5 nm. The results of measurements have shown a precise consistency between the simulated dynamical diffraction pattern and the observed diffraction pattern (Fig. 2c). Thus it is determined that the X phase has a C-centred orthorhombic crystal structure with a unit cell of Al:Cu:Mg = 2:4:4.

3.3. Orientation relationship between X phase and the matrix

Because the lattice structure of X phase has been determined, the orientation relationship between matrix and X phase could be calculated using the method mentioned in the previous section. According to Fig. 2 and Table III, we could find five specific orientation relationship which corresponded to different directions

(1) $(0\,1\,-1)_m \parallel (1\,1\,0)_X$; $[0\,1\,1]_m \parallel [1\,-1\,2]_X$

(2) $(0\,1\,-1)_m \parallel (0\,1\,0)_X$; $[0\,1\,1]_m \parallel [1\quad 0\,1]_X$

(3) $(1\,-1\,0)_m \parallel (0\,1\,0)_X$; $[0\,0\,1]_m \parallel [2\quad 0\,1]_X$

(4) $(1\,-1\,0)_m \parallel (1\,1\,0)_X$; $[0\,0\,1]_m \parallel [1\,-1\,1]_X$

(5) $(1\,-1\,0)_m \parallel (0\,1\,0)_X$; $[1\,1\,2]_m \parallel [1\quad 0\,2]_X$

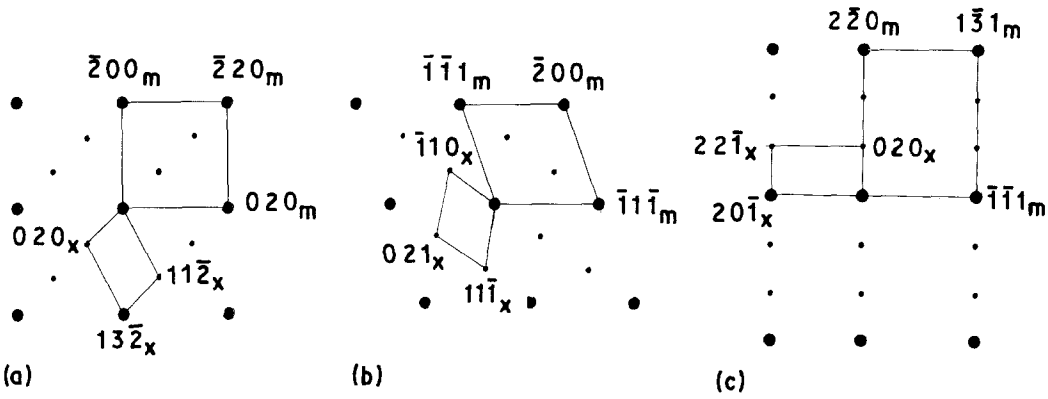

Figure 10 Schematic illustration of the indexed pattern of the SAD patterns of X phase in Fig. 2.

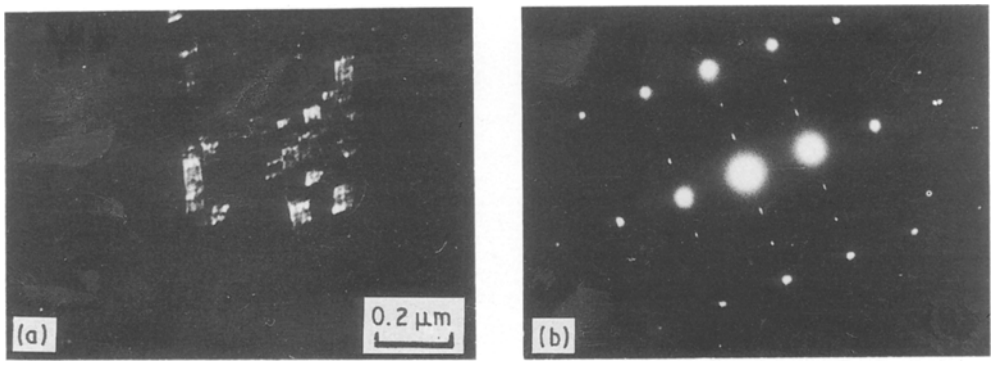

Figure 11 (a) Dark-field image of X phase and (b) corresponding SAD pattern in specimen B along the $[1\,1\,2]_m$ direction.

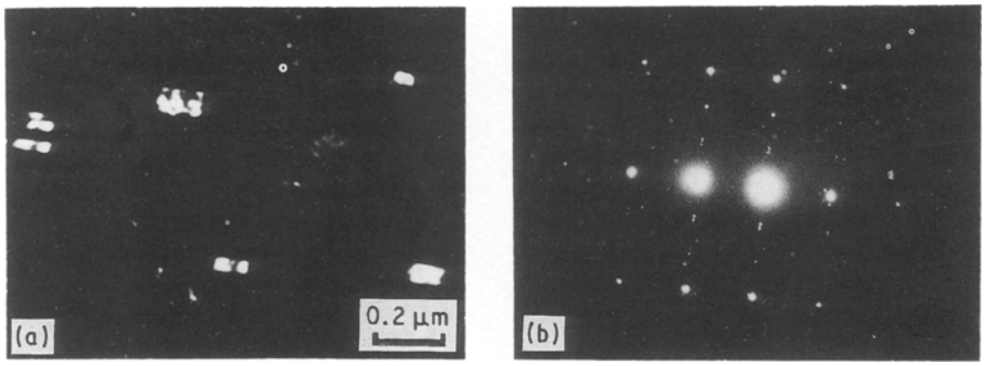

Figure 12 (a) Dark-field image of X phase and (b) corresponding SAD pattern in specimen c along the $[1\,1\,2]_m$ direction.

Through computer calculation, it is decided that the X phase has the typical orientation relationship $(1\,-1\,0)_m \parallel (0\,1\,0)_X$; $[-1\,-1\,-1]_m \parallel [0\,0\,1]_X$. The corresponding transformation matrix of direction indices is

$$B = \begin{bmatrix} 0.336 & 0.336 & -0.672 \\ 0.336 & -0.336 & 0.000 \\ -0.334 & -0.334 & -0.334 \end{bmatrix}$$

The indexed pattern of X phase along different matrix directions (Fig. 2) could then be decided as

$(1\,-1\,0)_m \parallel (0\,1\,0)_X$; $[0\,0\,1]_m \parallel [-2\,0\,-1]_X$

$(0\,-1\,2)_m \parallel (-1\,1\,0)_X$; $[0\,1\,1]_m \parallel [-1\,-1\,-2]_X$

$(1\,-1\,0)_m \parallel (0\,1\,0)_X$; $[1\,1\,2]_m \parallel [-1\,0\,-2]_X$

The indexed pattern is also schematically illustrated in Fig. 10.

3.4. Effect of ageing conditions on the precipitation of X phase

Figs 11a and 12a show the X phase observed in specimens B and C, respectively. Figs 11b and 12b are the corresponding SAD patterns. The electron beam was incident in the $[1\,1\,2]_m$ direction. The quantity of X phase is less than that of needle-like S′ phase. As revealed in Fig. 11, in the initial stage of precipitation, the X phase forms as a group of small plate-like precipitates. The corresponding diffraction spots are elongated along the $[0\,1\,0]_X$ direction. With the increase in ageing temperature, the X phase grows in size and splits into cuboid-like phase. At this stage, the double diffraction spots exist along the $[0\,1\,0]_X$ direction. At a very high ageing temperature (420 °C), the X phase will precipitate quickly into a bulk-like phase with crystal structure shown in Figs 1 and 2.

4. Conclusion

In the 2124 aluminium alloy, a new kind of precipitate phase (X phase) has been found, which is different from the S precipitate phase. The X phase has an orthorhombic crystal structure with $a = 0.492$ nm, $b = 0.852$ nm and $c = 0.701$ nm. The space group of the phase is Cmmm. There are 10 atoms in a unit cell with Al:Cu:Mg = 2:4:4. The X phase has the orientation relationship with matrix: $(1\,-1\,0)_m \parallel (0\,1\,0)_X$; $[-1\,-1\,-1]_m \parallel [0\,0\,1]_X$.

At low ageing temperatures, the X phase initially precipitates into a group of plate-like phases. With the increase in ageing temperature, the X phase grows into cuboid-like phase and finally forms bulk-like phase.

Acknowledgement

The Chinese Aeronautical Science Foundation are thanked for financial support.

References

1. J. E. HATCH, "Aluminum: Properties and Physical Metallurgy" (American Society for Metals, Metals Park, Ohio, USA, 1984) p. 189.
2. R. E. SANDERS, T. H. SANDERS and J. T. STALEY, *Aluminium* **59** (1983) 143.
3. A. K. GUPTA, P. GAUNT and M. C. CHATURVEDI, *Phys. Mag.* **55** (1987) 375.
4. S. HISASHI and K. MOTOHIRO, *J. Jpn Inst. Light Met.* **31** (1981) 277.
5. K. SHIGEYASU, *ibid.* **36** (1986) 525.
6. LI CHUNZHI and YAN MINGGAO, *Chinese J. Met. Sci. Tech.* **3** (1987) 27.

Received 12 September 1989
and accepted 26 October 1990